Digital Twin of Ventricular Activation Through Realistic Purkinje Network Calibrated to Clinical ECGs

Sandra Perez-Herrero[1], Jorge Sánchez[1], Ferran Prats-Domenech[2], Lucia Riaza-Martin[2], Ferran Roses-Noguer[2], Beatriz Trenor[1], Javier Saiz[1], Guadalupe García-Isla[1]

[1] Centro de Investigación e Innovación en Bioingeniería, Universitat Politècnica de València, Valencia, Spain
[2] Pediatric cardiology department, Hospital Universitario Vall d'Hebron, Barcelona, Spain

Abstract

The His–Purkinje system governs ventricular activation but cannot be directly characterized in vivo. We propose a framework to personalize ventricular digital twins from routine clinical data, combining computed tomography (CT) and electrocardiogram (ECG) records by optimizing His-Purkinje insertions. A 3D ventricular pediatric model was reconstructed, and candidate insertions sites were placed at the center of each American Heart Association (AHA) region. A genetic algorithm localized seven insertion sites, followed by temporal optimization of their activation delays with Bayesian optimization, both guided by the Dynamic Time Warping metric (DTW). Results showed that seven sites were sufficient to reproduce the patient's QRS morphology, achieving an average cross-correlation (CC) aligned to V1 of 0.73±0.045 through the 10^{th} percentile of the best solutions. Temporal optimization added little benefit, underscoring that spatial localization with synchronous stimulation is sufficient for clinical QRS reproduction. Our results indicate that different spatial locations can produce comparable QRS morphologies; however, inter-lead lagging is sometimes present and may persist or even increase in certain cases after temporal optimization.

1. Introduction

Synchronous electrical activation and mechanical contraction of the ventricular myocardium are orchestrated by the specialized His–Purkinje conduction system. Arising from the His bundle and bifurcating into the right and left bundle branches, this network rapidly distributes the depolarization wavefront through a fine endocardial arborization. Despite its pivotal role, the Purkinje network exhibits marked inter-individual variability in branching topology, endocardial coverage, and Purkinje–myocardial junctions (PMJs) density [1]. Such variability influences activation sequences, QRS morphology, ventricular synchrony, and response to therapies such as cardiac resynchronization or His-bundle / left bundle branch pacing. In recent years, cardiac digital twins (CDTs), patient-specific biophysical models that integrate multiscale and multiphysics dynamics, have recently emerged as a powerful advance for precision cardiology. As no method exists to reconstruct Purkinje topology in vivo [2], physiological simulated QRS are typically obtaining the propagation pattern from rule-based early activation sites [3]. Automated functional twinning, under these assumptions, cannot be reliably achieved the inter-individual variability [4]. Particularly in pediatric or pathological hearts subtle differences in myocardial structure can strongly influence QRS morphology. Other studies propose the personalization of root activation points for the patient [4, 5], although effective personalization remains challenging due to the ill-posed nature of parameter inference and the fact that clinical observations are often noisy and asynchronous.

In this study, we propose to construct patient-specific CDTs from routine clinical data, computed tomography (CT) and standard 12-lead ECGs, to infer the Purkinje-driven endocardial activation patterns. Our study aims to develop a framework that personalizes ventricular CDTs by first optimizing the spatial distribution of His-Purkinje insertions and subsequently optimizing their activation timings, with the goal of reproducing patient-specific QRS morphology and disentangling the relative contributions of spatial and temporal variability in endocardial activation.

2. Methods

2.1. Simulation Setup

A 3D hexahedral ventricular mesh (400 μm resolution) was reconstructed from CT images of a 15-year-old healthy female provided by Vall d'Hebron University Hospital. A Purkinje network (100 μm resolution) covering

uniformly the endocardial surface was generated with the method proposed by Costabal et al. [6]. ELVIRA monodomain solver [7] was used to perform electrophysiological simulations using the O'Hara–Rudy et al. [8] model for ventricle and Stewart et al. [9] model for Purkinje, with conduction velocities of 0.67 m/s and 2 m/s, respectively. ECGs were computed via an infinite volume conductor approach.

2.2. His-Purkinje Optimization

His bundle insertions to the Purkinje network (His-Purkinje insertions), are essential for initiating endocardial depolarization and shaping QRS morphology. One Purkinje internal node placed on the center of each American Heart Association (AHA) [10] region was chosen as candidate insertion point, and each one was assigned an individual activation time to capture physiological temporal delays [11]. QRS optimization was performed in two phases: first a spatial optimization (SO) to select the most accurate His-Purkinje insertion positions, and then a temporal optimization (TO) to refine their activation times (AT). To avoid initialization bias five different realizations were done with different random seeds. Personalization required 15 hours per seed on the Marenostrum 5.0 HPC system.

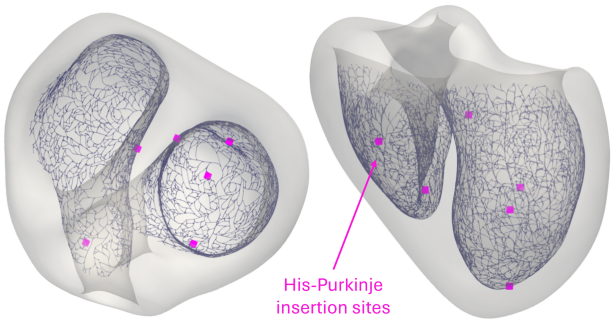

Figure 1. Model of Purkinje network with His-Purkinje insertion sites

2.2.1. Spatial Optimization

The SO initiated from a population of different combinations of 7 nodes locations, with 2 nodes in the right ventricle (RV) and 5 in the left ventricle (LV). Within each ventricle, a 30 mm inter-nodal distance was maintained.

Optimal positions were inferred using a genetic algorithm (GA) implemented in PyGAD [12], evolving 23 individuals over 12 generations. For each individual, a 12-lead ECG was computed after synchronous activation of the selected insertion points, focusing on the QRS complex and evaluated using Dynamic Time Warping metric (DTW) [5] to guide the optimization.

2.2.2. Temporal Optimization

Starting from the best SO inference for each seed, Bayesian optimization was applied over 60 iterations to refine the activation of the seven SO-inferred nodes. Delays were constrained between 1-21 ms, consistent with physiological endocardial activation [11]. DTW was used to guide the optimization.

2.3. Error Metrics

Three metrics were explored to assess similarity between simulated and clinical ECGs: DTW, mean cross-correlation (CC) aligned to V1, and a weighted combination (DWT-CC) defined in equation 1.

$$\mathcal{E}_{\mathcal{DTW}-\mathcal{CC}} = \lambda_{\text{DTW}}\mathcal{E}_{\mathcal{DTW}} + \lambda_{\text{CC}}(1-\mathcal{E}_{\mathcal{CC}}) \quad (1)$$

where $\mathcal{E}_{\mathcal{DTW}}$ and $\mathcal{E}_{\mathcal{CC}}$ are normalized values with respect to the best and worst outcomes among all simulations performed during SO. The weights λ_{DTW} and λ_{CC}, were set to 0.4 and 0.6, respectively.

While DTW captures morphological features, CC includes also temporal inter-lead misalignment.

After SO, the best 10^{th} percentile considering DTW–CC metric was selected, and the best inference per seed was then used for TO. DTW–CC was used to identify the optimal TO solution.

3. Results

3.1. Spatial Optimization

A total of 99 simulations comprised the top 10^{th} percentile of the DTW–CC distribution from SO, with an average DTW of 0.30 ± 0.04 and CC of 0.73 ± 0.045. Fig. 2 summarizes the AHA activation probability (AP). In the RV, high activation occurred at the origin (AHAs: 20, 26) and insertion (23, 29) of correspondent moderator band regions. In the LV, predominant activation was mainly in the septal (2, 3, 8, 9) and apical (14) regions, while medium AP appeared in the basal lateral areas (1, 4, 5, 6). AP was asymmetric across the septum.

Fig. 3 shows a heatmap of mean activation times with marks on AHA segments insertion sites inferred. In the RV (18-34), in seed 1 the first regions activated were the apex (30-34) and basal posterior free wall (21-22); in seed 2, the septal insertion of moderator band (25-26) and apex (30-34). Others seeds showed combinations of moderator band insertion regions (29,25,26), basal septum (20), and posterior free wall (21-23). In the LV (1-17), seeds 1 and 3 started activation in the apical septum (8, 9, 14); in seeds 4 and 5, it starts in septum (2,3,8,9,14), and seed 2 was similar to these but with added stimulation on anterior free

wall (12). In all cases, depolarization began in the apical RV and ended in the LV posterior free wall.

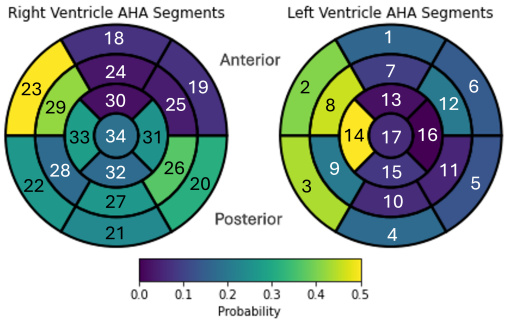

Figure 2. AP of 10th percentile of SO per AHA segment.

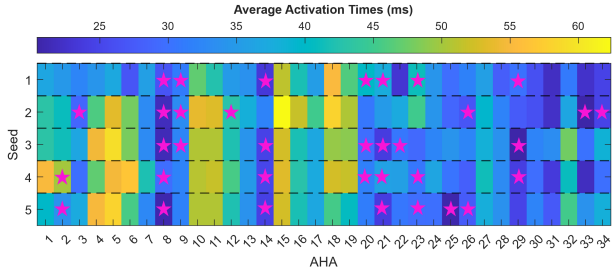

Figure 3. Average AT per AHA for the best SO solutions per seed. Starts mark inferred His-Purkinje insertions.

3.2. Temporal Optimization

Fig. 4 shows the simulated ECG for both the SO and the TO over the clinical ECG for seed 3. Table 1 summarizes the best metrics obtained for each initialization seed after SO alone and after including TO. TO generally improved DTW values, indicating a closer morphological match with the patient's QRS. However, CC did not consistently increase, and in the majority of cases even decreased, leading to a worse combined DTW–CC score for all seeds.

	SO			TO		
Seed	DTW	CC	DTW-CC	DTW	CC	DTW-CC
1	0.23	0.73	0.03	0.29	0.75	0.07
2	0.25	0.74	0.03	0.21	0.73	0.04
3	0.25	0.80	0.01	0.20	0.72	0.03
4	0.29	0.79	0.03	0.20	0.63	0.08
5	0.27	0.80	0.02	0.29	0.72	0.09

Table 1. Metrics for the best SO and their TO per seed.

4. Discussion

Seven His-Purkinje insertion sites were sufficient to reproduce the patient's QRS, with most optimal configurations having four sites in the LV and three in the RV, consistent with previous studies [3]. As illustrated in Fig. 2, the 10th percentile of the top spatial inferences generated a probabilistic activation map that aligned with the known spatial distribution of the Purkinje PMJs [1]. This shows that, even without prior knowledge, our framework could infer key activation sites possibly reflecting patient-specific variations based solely on QRS and ventricular anatomy. These maps could guide functional Purkinje network modeling and the asymmetric PMJs distribution.

Analysis of the best solutions for each seed (Fig. 3) shows that, despite different starting points and simultaneous activation of all inferred sites, electrical propagation present the physiologically expected pattern [11]. This behavior probably results from the combined effect of well-localized His-Purkinje insertion nodes, ventricular anatomy, and differences in mass distribution. Regarding TO, we observed in Table 1 that it could improve DTW, enhancing morphological alignment but decreasing the overall CC, reflecting individual lead morphological worsening or temporal lagging across leads. These discrepancies underscored the need for an appropriate error metric; here, we combined two common ones to balance morphological and temporal features. Taking this into account, TO did not yield consistent improvement over synchronous stimulation, as can be appreciated in Fig. 4. This emphasizes that correct spatial localization with synchronous activation is sufficient for physiologically reasonable QRS morphology reproduction. Similar results were reported by Cardone et al. [3] and Camps et al. [5], while Gillette et al. [4] achieved this by pre-excitating only the moderator band insertion site. Nevertheless, we directly addressed the effect of inter-lead temporal lagging of the SO and posterior TO outcome by comparing DTW, CC and DTW-CC.

It is known that multiple Purkinje configurations can simulate QRS highly consistent with clinical recordings [2], and our results show that the same Purkinje network with different spatial arrangements of His–Purkinje insertions can reproduce equivalent ECGs, highlighting the intrinsic uncertainty and the need to consider multiple plausible configurations when personalizing CDTs.

Future work could leverage alternative approaches such as Eikonal model and lead-field ECG computation [4] to achieve a faster optimization. Additionally, applying the pipeline to a 3D population of patient-specific models would help validate its robustness and potential clinical utility. Moreover, future studies should focus on quantifying the uncertainty inherent to Purkinje network modeling.

5. Conclusion

We present a pediatric ventricular CDT calibrated to clinical 12-lead ECG. Our results indicate that a limited number of His-Purkinje insertions synchronously stimu-

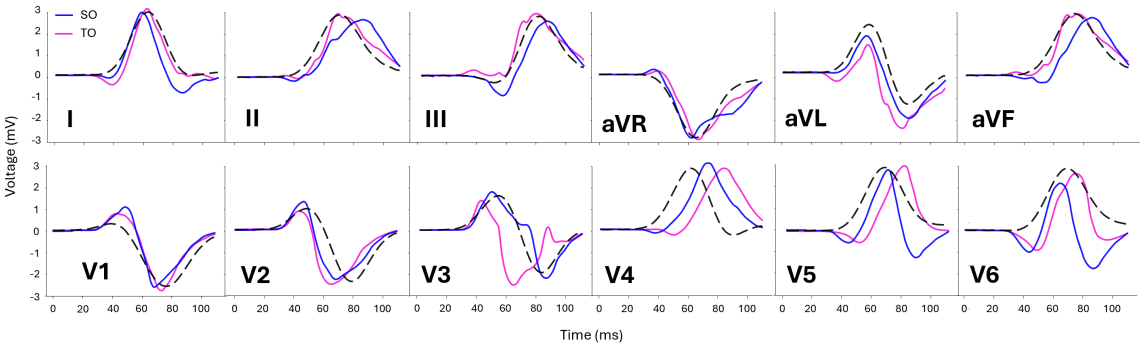

Figure 4. Spatial optimization (blue), Temporal optimization (pink) and clinical QRS (black) for seed 3 top result.

lated can reproduce QRS morphology, and multiple spatial configurations yield comparable outcomes, highlighting the uncertainty during His-Purkinje system modeling.

Acknowledgments

This work was partially supported by the Dirección General de Política Científica de la Generalitat Valenciana (CIPROM/2023/14), Ayuda a Primeros Proyectos de Investigación (PAID-06-24), Vicerrectorado de Investigación de la Universitat Politècnica de València (UPV), Juan de la Cierva 2022 grant from Plan Estatal de Investigación Científica y Técnica y de Innovación 2021-2023, funded by NextGenerationEU and by the grant PID2022-140553OB-C41supported by MICIU/AEI/10.13039/501100011033 and by FEDER/UE. The author thankfully acknowledges RES resources provided by Barcelona Supercomputing Center in MareNostrum5 to IM-2024-1-0010, IM-2024-2-0015, IM-2024-3-0001, IM-2025-1-0010 and IM-2025-2-0007.

References

[1] Sebastian R, Zimmerman V, Romero D, Sanchez-Quintana D, Frangi AF. Characterization and Modeling of the Peripheral Cardiac Conduction System. IEEE Transactions on Medical Imaging 2012;32(1):45–55.

[2] Álvarez Barrientos F, Salinas-Camus M, Pezzuto S, Sahli Costabal F. Probabilistic Learning of the Purkinje Network from the Electrocardiogram. Medical Image Analysis 2025; 101:103460. ISSN 1361-8415.

[3] Cardone-Noott L, Bueno-Orovio A, Mincholé A, Zemzemi N, Rodriguez B. Human Ventricular Activation Sequence and the Simulation of the Electrocardiographic QRS Complex and its Variability in Healthy and Intraventricular Block Conditions. EP Europace 12 2016;18:iv4–iv15.

[4] Gillette K, Gsell MA, Prassl AJ, Karabelas E, Reiter U, et al. A Framework for the Generation of Digital Twins of Cardiac Electrophysiology from Clinical 12-Leads ECGs. Medical Image Analysis 2021;71:102080. ISSN 1361-8415.

[5] Camps J, Lawson B, Drovandi C, Minchole A, Wang ZJ, Grau V, et al. Inference of Ventricular Activation Properties from Non-Invasive Electrocardiography. Medical Image Analysis 2021;73:102143. ISSN 1361-8415.

[6] Sahli Costabal F, Hurtado DE, Kuhl E. Generating Purkinje Networks in the Human Heart. Journal of Biomechanics 2016;49(12):2455–2465. ISSN 0021-9290. Cardiovascular Biomechanics in Health and Disease.

[7] Heidenreich EA. Algoritmos para Ecuaciones de Reacción Difusión Aplicados a Electrofisiología. Ph.D. thesis, 2009.

[8] O'Hara T, Virág L, Varró A, Rudy Y. Simulation of the Undiseased Human Cardiac Ventricular Action Potential: Model Formulation and Experimental Validation. PLoS Computational Biology 2011;7(5):e1002061.

[9] Stewart P, Aslanidi OV, Noble D, Noble PJ, Boyett MR, Zhang H. Mathematical Models of the Electrical Action Potential of Purkinje Fibre Cells. Philosophical Transactions of the Royal Society A Mathematical Physical and Engineering Sciences 2009;367(1896):2225–2255.

[10] Cerqueira MD, Weissman NJ, Dilsizian V, Jacobs AK, Kaul S, Laskey WK, et al. Standardized Myocardial Segmentation and Nomenclature for Tomographic Imaging of the Heart: A Statement for Healthcare Professionals from the Cardiac Imaging Committee of the Council on Clinical Cardiology of the American Heart Association. Journal of Nuclear Cardiology 2002;9(2):240–245. ISSN 1071-3581.

[11] Durrer D, Dam RTV, Freud GE, Janse MJ, Meijler FL, Arzbaecher RC. Total Excitation of the Isolated Human Heart. Circulation 1970;41(6):899–912.

[12] Gad AF. Pygad: An Intuitive Genetic Algorithm Python Library. Multimedia Tools and Applications 2023;1–14.

Address for correspondence:

Sandra Perez-Herrero
Centro de Investigación e Innovación en Bioingeniería (Ci2B), Universitat Politècnica de València, Camino de Vera s/n, 46022 Valencia, Spain
sanpeher@ci2b.upv.es